

Dual Drug Loaded Lipid Nanocarrier Formulations for Topical Ocular Applications

Ahmed Adel Ali Youssef^{1,2}, Narendar Dudhipala², Soumyajit Majumdar^{2,3}

¹Department of Pharmaceutical Technology, Faculty of Pharmacy, Kafrelsheikh University, Kafrelsheikh, 33516, Egypt; ²Department of Pharmaceutics and Drug Delivery, School of Pharmacy, University of Mississippi, Oxford, MS, 38677, USA; ³Research Institute of Pharmaceutical Sciences, University of Mississippi, Oxford, MS, 38677, USA

Correspondence: Soumyajit Majumdar, Department of Pharmaceutics and Drug Delivery, School of Pharmacy, University of Mississippi, 113J TCRC West, Oxford, MS, 38677, USA, Tel +1 662 915-3793, Email majumso@olemiss.edu

Introduction: Untreated ocular infections can damage the unique fine structures of the eye with possible visual impairments and blindness. Ciprofloxacin (CIP) ophthalmic solution is prescribed as first-line therapy in ocular bacterial infections. Natamycin (NT) ophthalmic suspension is one of the progenitors in ocular antifungal therapy. Nanostructured lipid carriers (NLCs) have been widely examined for ocular penetration enhancement and distribution to deeper ocular tissues. The objective of the current study was to prepare NLCs loaded with a combination of CIP and NT (CIP-NT-NLCs) and embed them in an in-situ gelling system (CIP-NT-NLCs-IG). This novel formulation will target the co-delivery of CIP and NT for the treatment of mixed ocular infections or as empirical treatment in case of limited access to healthcare diagnostic services.

Methods: CIP-NT-NLC and CIP-NT-NLC-IG formulations were evaluated based on physicochemical characteristics, in vitro release, and ex vivo transcorneal permeation studies and compared against commercial CIP and NT ophthalmic eye drops.

Results and Discussion: NLCs formulation (0.1% CIP and 0.3% NT) showed particle size, polydispersity index, and zeta potential of 196.2 ± 1.2 nm, 0.43 ± 0.06 , and -28.1 ± 1.4 mV, respectively. Moreover, CIP-NT-NLCs showed entrapment efficiency of 80.9 ± 2.9 and $98.7 \pm 1.9\%$ for CIP and NT, respectively. CIP-NT-NLCs-IG formulation with 0.2% w/v gellan gum demonstrated the most favorable viscoelastic characteristics for ocular application. CIP-NT-NLCs and CIP-NT-NLCs-IG formulations exhibited a sustained release pattern for both drugs over 24 h. Moreover, CIP-NT-NLCs and CIP-NT-NLC-IG formulations showed 4.0- and 2.2-folds, and 5.0- and 2.5-folds enhancement in ex vivo transcorneal permeability of CIP and NT, respectively, compared to the control formulations.

Conclusion: The results suggest that this dual nanoparticulate-based in-situ gelling drug delivery system can serve as a promising topical delivery platform for the treatment of ocular infections.

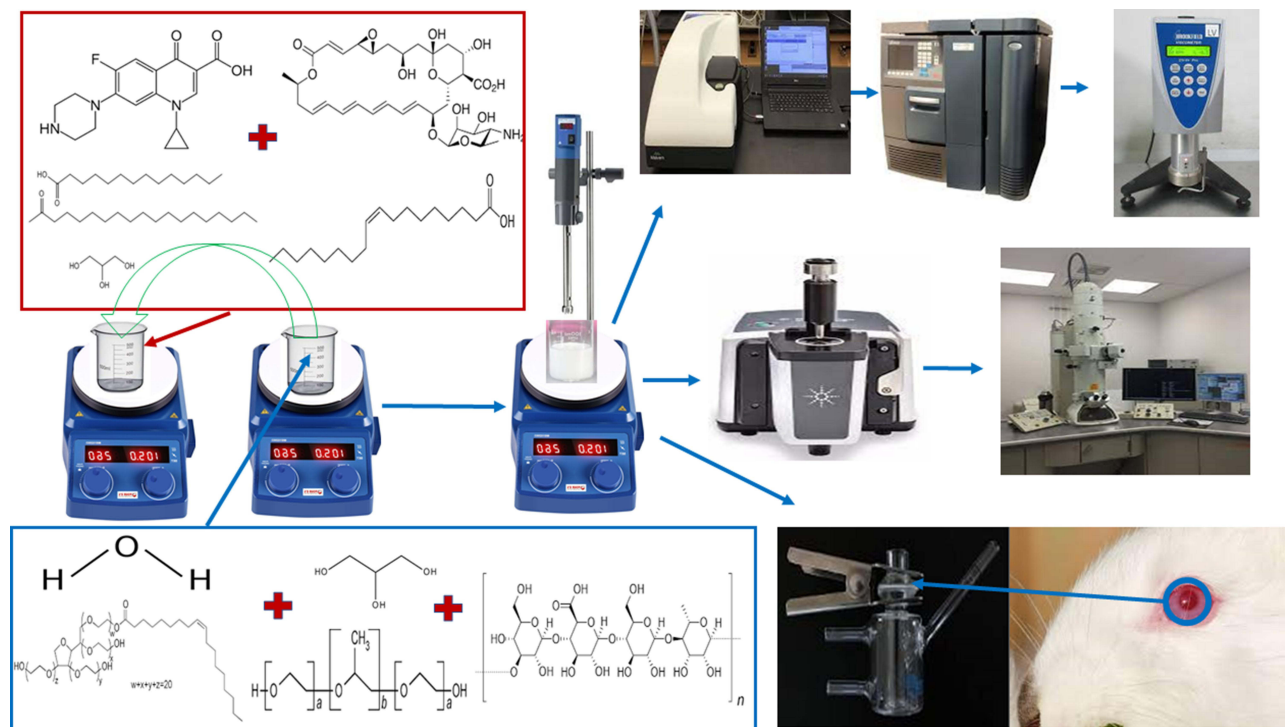
Keywords: keratitis, ciprofloxacin, natamycin, dual, nanostructured lipid carriers, sustained, in-situ gel, stability, transcorneal flux, permeability

Introduction

Microbial keratitis (MK) is defined as a nonviral corneal infection, caused by bacteria, fungi, and/or protozoa.¹ MK is an emergency that could result in vision loss for which the prospect of visual rehabilitation is often poor.¹ Global estimates of MK as a cause of unilateral blindness range from 1.5 to 2 million cases per year, although this figure is likely conservative due to underreporting in developing countries.¹ MK results in approximately 1 million clinical visits per year to healthcare practitioners and 58,000 registered emergency departments in the USA.¹ In addition, MK costs the US healthcare system an estimated 175 million US dollars in direct health expenditures, and approximately 70 million dollars in Medicare and Medicaid-related costs.^{1,2}

Corneal infection induced by more than one microorganism occurs as a result of co-infection, or as a secondary infection on top of an existing microorganism.³ Multiple investigations, performed in different areas of the world, have reported a high incidence rate of ocular co-infection by bacteria and fungi.³⁻⁷ According to a 10-year study at a tertiary referral center in the USA, a relatively high incidence rate of mixed bacterial-fungal infections was reported.⁸ Therefore,

Graphical Abstract



the possibility of a co-infection by bacterial and fungal microorganisms should be considered. Thus, the objective of the current study was to develop a dual drug-loaded formulation for the treatment of mixed bacterial and fungal ocular infections and use as an empirical therapy to delay the rapid progression of infections in cases of limited access to proper diagnostic tools eg, in low and middle-income countries.

Natamycin (NT) is the only commercially available broad-spectrum polyene topical antifungal (Natacyn[®] eye drops) used as a first-line antifungal agent. Although NT eye drops have been existing in the market for almost 40 years, NT demonstrates low pre-corneal retention and a 2.0% ocular bioavailability (BA) only.⁹ Therefore, NT eye drops require frequent administration: one drop is instilled in the *conjunctival sac* every 1- to 2- h for the first 3–4 days and then reduced to one-drop 6–8 times daily for 14–21 days or until clinical resolution of active fungal keratitis.⁹ This dosage regimen could reduce patient compliance. Moreover, NT eye drops have been reported to cause side effects such as allergic reaction, chest pain, dyspnea, corneal opacity, eye edema, eye discomfort, eye irritation, eye hyperemia, foreign body sensation, eye pain, paresthesia, and tearing.¹⁰

Ciprofloxacin (CIP) is a broad-spectrum fluoroquinolone bactericidal antibiotic. It targets two topoisomerase enzymes involved in bacterial DNA synthesis, DNA gyrase and DNA topoisomerase IV. It is active against aerobic gram-positive and gram-negative bacteria, and is, thus, effective in the treatment of a wide variety of ocular bacterial infections.¹¹ CIP is available for ocular administration as ophthalmic solutions and ointments (0.3% w/v CIP base). Commercial CIP ophthalmic solution (Ciloxan[®]) requires frequent administration due to poor ocular BA while blurred vision, itching, redness, eye discomfort, and dryness are associated with the ocular application of the ointment.¹² The patient information leaflet for Ciloxan[®] eyedrops state that the dosing (continued during the nighttime) is as follows: 2 drops are instilled in the conjunctival sac every 15 min for the first 6 hours, followed by 2 drops every 30 min during the first day and reduced to two drops every hour during the second day, and then 2 drops every 4 h for other 12 days during corneal ulcer treatment. Based on the clinical response, the doctor will advise the patient if the treatment needs to be continued for

longer than 14 days or discontinued. For other bacterial infections, the dosing regimen is 1 or 2 drops 4 times a day; however, for severe infections, the dose for the first 2 days may be increased to 1 or 2 drops every 2 h, while the patient is awake. Thus, the recommended dosage regimen, similar to NT, is not patient-friendly. Moreover, the solubility of CIP is low at tear fluid pH, and precipitation can take place upon installation of the commercial ophthalmic solution, leading to reduced efficacy and ocular BA of this drug.¹³

The epidemiology of MK has been investigated through the analysis of microorganisms cultured from corneal tissue. Based on the literature review, the most frequently implicated microorganisms in MK are *Staphylococcus* and *Pseudomonas* species for bacteria and *Candida* and *Fusarium* species for fungus.^{14,15} NT is preferred over other antifungal agents because of its activity against ocular infections caused by filamentous fungi, its safety, and its effectiveness at low concentrations.⁹ CIP is prescribed in the treatment of bacterial keratitis,¹⁶ endophthalmitis,¹⁷ bacterial and allergic conjunctivitis,¹⁸ and many other bacterial infections of the eye. Moreover, CIP has been reported to enhance the activity of many antifungal drugs better than other fluoroquinolones against *Candida albicans* and *Aspergillus fumigatus*.¹⁹ Therefore, CIP and NT were selected for the development of the dual drug-loaded nanostructured lipid carriers (NLC) formulation.

Topical ocular administration is the most widely accepted non-invasive route of drug administration to treat ocular infections because of ease of administration and patient compliance.¹² However, reflex blinking, tear turnover, tear dilution, and nasolacrimal drainage are physiological and anatomical ocular barriers that limit the delivery of therapeutic agents to their intraocular destination through the topical route.^{16,17} Novel nanotechnology-based drug delivery systems for improving penetration through these barriers have been widely examined.^{10,13,20–22} Lipid nanocarriers are easy to prepare, biocompatible, nonirritant, sustain drug release, and have been reported to improve ocular penetration of many active pharmaceutical ingredients.^{23,24} NLCs have been developed as second-generation lipid-based nanoparticles to overcome the drawbacks of low entrapment efficiency (EE) and drug expulsion on storage associated with solid lipid nanoparticles (SLNs).^{25,26} A less ordered solid lipid matrix structure that is created by the addition of a liquid lipid to the solid lipid, to convert SLNs to NLCs, is the main factor behind increasing drug load within the formulation and improving stability during storage.²⁷

In-situ gelling (IG) systems are in the solution state at the time of topical application but undergo sol-to-gel transformation upon contact with the physiological fluids or mucosa.²² Sol-to-gel phase transition, triggered by different physicochemical stimuli that are physiologically present on the ocular surface such as temperature, ionic strength, and pH, is the main advantage of their use.²² Prolonged ocular surface retention can improve the ocular BA of drugs and lead to better therapeutic outcomes.^{20,21} Furthermore, reducing the precorneal removal of the gel decreases the absorption into systemic circulation during ocular administration and thereby lowers the risk of side effects.²¹

The present study aimed to develop dual drug-loaded NLCs (CIP-NT-NLCs) and NLC-IG (CIP-NT-NLC-IG) formulations, using ion-sensitive IG agent, to enhance pre-corneal retention, ocular penetration, and to enhance the therapeutic outcomes, with concurrently reduced drug exposure, for the treatment of mixed bacterial and fungal ocular infections. Accordingly, CIP-NT-NLCs were prepared and characterized based on the physicochemical parameters such as particle size, polydispersity index, and zeta potential and subjected to a three-month stability study. CIP-NT-NLCs were then converted into an IG system (CIP-NT-NLC-IG) by the addition of gellan gum. CIP-NT-NLCs and CIP-NT-NLCs-IG formulations were further evaluated for stability, in vitro release, and ex vivo transcorneal permeation studies using commercial dosage forms as a control.

Materials

NT was purchased from Cayman Chemicals (Ann Arbor, MI, USA). CIP base (CAS number: 85721-33-1) was obtained from Sigma Aldrich (St. Louis, MO). Glyceryl distearate (Precirol® ATO 5) was a generous gift sample from Gattefossé (Paramus, NJ, USA). Poloxamer 188, oleic acid, castor oil, Polysorbate 80, Amicon® Ultra centrifugal filter devices with regenerated cellulose membrane (molecular weight cut off 100 kDa), 0.5 mL cup-like design Thermo Scientific™ Slide-A-Lyzer™ MINI Dialysis Device (10K molecular weight cutoff) and High Performance Liquid Chromatography (HPLC) grade solvents were acquired from Fischer Scientific (Hampton, NH, USA). Gellan gum was obtained from MP Biomedicals, LLC (Santa Ana, CA, USA). Centrifuge tubes, HPLC vials, and scintillation glass vials were obtained

from Fischer Scientific (Hampton, NH, USA). The whole eyes of male albino New Zealand rabbits were obtained from Pel-Freez Biologicals (Rogers, AR, USA).

HPLC Method for in vitro Sample Analysis

Samples were analyzed for CIP base and NT content using an HPLC-UV method. The HPLC system consisted of a Waters 717 plus auto-sampler coupled with a Waters 2487 Dual λ Absorbance UV detector, and an Agilent 3395 Integrator. The mobile phase consisting of a mixture of phosphate buffer (25 mM, pH of 2.4 adjusted using NaOH solution) and acetonitrile (70:30), was pumped at 1 mL/min flow rate through C18 Phenomenex Luna[®] (5 μ m, 250 \times 4.6 mm) column. The temperature for this analysis was set at 25°C, the injection volume was 20 μ L, and the UV detection wavelength was set to 290 nm. The method was found to be linear over a CIP base and NT concentration range of 1–30 μ g/mL. The validation of the analytical method was included as a supplementary (Table S1 and Figure S1) report with the manuscript.

Preparation of CIP-NT-NLCs

NLC formulations were prepared by the homogenization method.¹⁷ Briefly, solid and liquid lipid were melted at $80.0 \pm 2.0^\circ\text{C}$. Accurately weighed amount NT was added in small portions followed by CIP base to prepare the oily phase. An aqueous phase, containing surfactants (Poloxamer 188 and Polysorbate 80) and glycerin in Milli-Q water, was also heated at $80.0 \pm 2^\circ\text{C}$. Then, the hot aqueous phase was added dropwise to the molten oily phase under continuous magnetic stirring at 2000 rpm for 10 min to form a coarse emulsion. Using a T25 digital Ultra-Turrax (IKA, Germany) at 15,000 rpm for 5 mins ($65 \pm 2^\circ\text{C}$), the coarse emulsion was further emulsified to form a hot nanoemulsion. Cooling this nanoemulsion to room temperature resulted in the formation of the NLC colloidal dispersion. Production parameters like different homogenization speeds, different ratios of total lipids to surfactant, and different primary surfactant concentrations (Polysorbate 80) in the formulation were tested during the preparation of NLC placebos. Other parameters like mixing time and homogenization time were selected based on earlier reported studies.¹⁷

Preparation of CIP-NT-NLC-IG

The NLCs preparation method, as described above, was also followed for the preparation of IG formulations. However, the volume of water used to prepare NLCs was split into two equal parts: one part was used to prepare the aqueous solution of gellan gum, and the other half was used to prepare the aqueous solution of surfactants as described above.

Control Formulations

CIP Hydrochloride Ophthalmic Solution Control (CIP-HCl-C)

CIP hydrochloride ophthalmic solution (Ciprofloxacin Ophthalmic Hydrochloride Solution, 0.3% as a base, Alcon Laboratories, Texas, USA; Lot # 295240F) was diluted using Dulbecco's phosphate-buffered saline (DPBS, pH 7.2) to ensure concentration of CIP base in the control (CIP-HCl-C) and test formulations were equal.

NT Ophthalmic Suspension (NT-C)

NT ophthalmic suspension (Natacyn[®], 5.0% w/v, Alcon Laboratories, Texas, USA; Lot # 271802F) was also diluted with DPBS to ensure concentration of NT in the control (NT-C) and test formulations were equal.

Characterization of NLCs

Particle Size (PS), Polydispersity Index (PDI), and Zeta Potential (ZP)

Photon correlation spectroscopy using Zetasizer (Nano ZS Zen3600, Malvern Panalytical Inc., Westborough, MA, USA) was used for PS, PDI, and ZP measurement of the nanodispersions at room temperature (25°C) in disposable, solvent resistant, micro cuvette (ZEN0040). The cuvette was flushed out with 0.22 μ m filtered Milli-Q water before sample loading to ensure the absence of dust/particulates in the cuvette before measurement. PS and PDI were analyzed based on volume distribution. ZP measurement was performed on the same diluted samples. The samples were further diluted 100 times with Milli-Q water to avoid multi-scattering phenomena. All measurements were carried out in triplicate.

CIP and NT Content (Assay)

CIP and NT content in the CIP-NT-NLCs formulations were determined by the lipid precipitation method.^{9,13} For CIP content analysis, 10 µL NLC formulation was mixed with a 990 µL solvent mixture (0.1N HCl and ethanol (1:1)). For NT content determination, an accurately measured volume of the NLC formulation (10 µL) was extracted in methanol (990 µL). The mixtures were then centrifuged (AccuSpin 17R centrifuge, Fisher Scientific, USA) at room temperature for 20 mins at 13,000 rpm, and the supernatant was collected and analyzed for CIP and NT content following appropriate dilution using HPLC. All measurements were conducted in triplicates.

Entrapment Efficiency (EE)

The EE of CIP and NT in the CIP-NT-NLCs formulation was determined by quantifying the amount of untrapped drug in the aqueous phase of the nanocarriers. The EE was evaluated by an ultrafiltration technique with a 100 kDa centrifugal filter device (Amicon Ultra). Formulation (500 µL) was added to the sample reservoir and centrifuged for 20 mins at 13,000 rpm. The filtrate was analyzed for both drugs using HPLC following appropriate dilution. All measurements were carried out in triplicates, and the % EE was calculated by using the following equation (Eq.1):

$$\% EE = \left[\frac{W_a - W_f}{W_i} \right] \times 100 \quad (1)$$

Where W_a = amount of drug (CIP or NT) determined in the assay, W_f = amount of free drug (CIP or NT) in the aqueous phase, and W_i = initial amount of drug (CIP or NT) weighed.

Drug-Excipient Compatibility Study – Fourier Transform Infrared Spectroscopy (FTIR)

The infrared spectra of the samples were obtained using an Agilent Cary 660 FTIR Spectrometer (Agilent Technologies, Santa Clara, CA) in the wavelength range of 800–4000 cm^{-1} . Pure drugs, lipid excipients along with their physical mixture, placebo, and CIP-NT-NLCs formulation were studied for any drug-excipients incompatibility. The bench was equipped with a MIRacle Attenuated Total Reflection (Pike Technologies MIRacle ATR, Madison, WI), which was fitted with a single-bounce, diamond-coated ZnSe internal reflection element.

Characterization of NLC-IG

In vitro Gelling Characteristics of NLC-IG Formulations

The gel formation time (GT) is the time needed for IG formulations to change from a free-flowing liquid to a gel, without agitation, upon contact with simulated tear fluid (STF). The time needed for the gel to dissolve or break, recorded based on visual inspection every hour for the first 8 h and then every 4 h for the rest of the experiment, was considered as the gel residence time (GRT). STF with a pH of 7.0 ± 0.2 was prepared by adding 0.0084% calcium chloride, 0.138% potassium chloride, 0.678% sodium chloride, and 0.218% sodium bicarbonate, in deionized water, and was used as a medium for evaluation of the rheological behaviour.¹⁷ The GT and GRT of the formulations with different gellan gum concentrations were determined by adding the formulation (50 µL) to freshly prepared STF (2 mL) in glass vials maintained at $34.0 \pm 1.0^\circ\text{C}$ in a shaking water bath (PrecisionTM, Fisher Scientific, USA) operated for 24 h at 100 rpm.

Viscosity of NLC-IG Formulations

Brookfield cone and plate viscometer (LV-DV-II+ Pro Viscometer, Middleboro, USA) was used to measure the viscosity (η) of all IG formulations using a CPE 52 spindle operated at 10 rpm. Each IG formulation (1.0 mL) was placed in the viscometer cup plate in the absence and presence of STF. STF was added to the formulation in a ratio of 7:50 (0.14:1.0 mL) to measure the viscosity of the formed gel after topical application. The formulation to STF ratio was selected based on that a standard eyedropper dispenses 0.05 mL (50 µL) per drop and nasolacrimal drainage helps to maintain a precorneal fluid volume of about 7 to 10 µL at any time.²⁸ The temperature of the cup was maintained at 34°C using a circulating water bath. The viscosity measurement of all IG formulations was carried out in triplicates.

Surface Morphology—Transmission Electron Microscopy (TEM)

The analysis was performed using a JEOL 1400-Flash transmission Electron Microscope (JEOL, Peabody, MA, USA). TEM samples were examined according to a negative staining protocol with a solution of UranylLess. A carbon-plated copper grid was placed above one drop (20 μ L) of the formulation for 60 sec and the excess sample was removed with the aid of a filter paper after grid removal from the formulation surface. Next, the grid was placed above one drop (20 μ L) of the staining solution for 60 sec, and the excess stain was also drawn off the grid with the aid of a filter paper. The grid was then allowed to dry for a few minutes by air. The grid was examined under the transmission electron microscope.

In vitro Release from NLC and NLC-IGformulations

Based on the solubility reports of NT and CIP in different dissolution media, IPBS (pH 7.4) containing 2.5% w/v randomly methylated beta-cyclodextrin (RM β CD) was selected as the dissolution medium for the in vitro release studies.^{9,13} In vitro release profiles of CIP and NT from CIP-HCL-C, NT-C, CIP-NT-NLC, and NLC-IG formulations were evaluated using the diffusion method. Formulation (200 μ L) was added to the donor compartment (0.5 mL cup-like design Thermo Scientific™ Slide-A-Lyzer™ MINI Dialysis Device, 10K molecular weight cutoff), mounted on the top of a 20 mL scintillation glass vial (receiver compartment). STF was added along with the NLC-IG formulations inside the donor compartment at a ratio of 7:50 to form a gel. The content of the receiver compartment was maintained under continuous magnetic stirring at 34°C. Samples (1 mL) were removed from the receiver compartment and replenished with an equivalent volume of freshly prepared dissolution medium at pre-determined time points (0.5, 1, 2, 3, 4, 6, 8, 12, and 24 h). Samples were quantified using HPLC. The NT and CIP release data were analyzed for release kinetics using Microsoft (MS) Office excel statistical functions (Office 365, 2016, USA), and fitted to different mathematical models to understand the possible release mechanism.

Ex vivo Transcorneal Permeation Studies

Transcorneal permeation of NT and CIP from the NLC, NLC-IG, CIP-HCL-C, and NT-C formulations were performed on corneas isolated from rabbit whole eyes. The eyes were kept under cold condition in Hanks' balanced salt solution and shipped overnight, and immediately upon their arrival, the corneas were carefully excised and used for permeation studies. The isolated corneas were washed in IPBS solution, pH 7.4. The cornea was clamped in between the two chambers of the vertical diffusion cells (PermeGear® Inc., Hellertown, PA, USA) with the epithelial surface facing the donor chamber which contains test or control formulations. Thirty microliters of STF were added to the NLC-IG formulation (200 μ L) in the donor compartment to form a gel on the corneal surface, mimicking in vivo conditions. The content of the receiver chamber (5.0 mL of 2.5%w/v solution of RM β CD in IPBS; pH 7.4) was maintained under continuous magnetic stirring and the temperature was kept at 34°C with the aid of a circulating water bath. Samples (0.5 mL) were collected from the receiver chamber at pre-determined time points and replaced with an equivalent volume of the receiver medium. The samples were quantified using the HPLC method mentioned above. The cumulative amount of drug permeated (Q_n), steady-state flux (J_{ss}), and transcorneal permeability coefficient (P_{eff}), across the isolated rabbit cornea, were calculated to study the transcorneal permeation of CIP and NT. All samples were analysed in triplicates. Q_n was calculated using the following equation (Eq.2):

$$Q_n = V_r C_{r(n)} + \sum_{x=1}^{x=n} V_{s(x-1)} C_{r(x-1)} \quad (2)$$

Where, n is the sampling time point; V_r is the volume in the receiver compartment (mL), V_s is the volume of the Aliquot collected at the nth time point (mL) and $C_{r(n)}$ is the drug concentration in the receiver compartment at the nth time point (μ g/mL).

The rate of transcorneal permeation (dQ/dt) was calculated using the slope of Q_n versus the time plot. J_{ss} of the drug was determined using the following equation (Eq.3):

$$J_{ss} = (dQ/dt)/A \quad (3)$$

Where Q is the amount of drug transported and A is the effective area of permeation (0.636 cm²).

The permeability of the drug was calculated by the following equation (Eq.4):

$$P_{eff} = J_{ss}/C_0 \quad (4)$$

Where C_0 is the initial donor concentration for CIP or NT.

Stability Studies of CIP-NT-NLCs and CIP-NT-NLC-IG

The stability of NLC and NLC-IG formulations were evaluated at refrigerated (RF, $4 \pm 2^\circ\text{C}$, NLC only) and room temperature (RT, $25 \pm 2^\circ\text{C}$) storage conditions. Briefly, 10mL of NLC or NLC-IG dispersions were filled into 20 mL scintillation glass vials. The CIP-NT-NLCs formulation was evaluated for any change in PS, PDI, ZP, drug content (CIP and NT), and % EE (CIP and NT) at predetermined time intervals over three months. NLC-IG formulation was evaluated based on the changes in GT, GRT, and η with and without STF addition during one-month storage.

Statistical Analysis

SPSS software (IBM SPSS Statistics software, SPSS 28, USA) was used for statistical analysis of data. Statistically significant difference between the data was compared at a “p” value less than 0.05 ($p < 0.05$).

Results and Discussions

Preparation and Physical Characterization of NLC Placebos

Two different NLC placebo formulations were prepared using glyceryl distearate (solid lipid), castor oil (liquid lipid), and oleic acid (liquid lipid), selected based on the lipid solubility profile of CIP and NT in our earlier investigations.^{9,13,16,17} Surfactants (Poloxamer 188 and Polysorbate 80) and glycerin (2.25% w/v, tonicity adjusting agent) were used to prepare the aqueous phase. Many trials were performed to develop NLC formulations based on two different liquid lipids, different lipid to surfactant ratios, testing different concentrations of Polysorbate 80, and variation in homogenization speed.

Effect of Polysorbate 80 concentration

Polysorbate 80 has been reported to be the primary surfactant in the preparation of NLC formulations. Therefore, the effect of different concentrations of Polysorbate 80 on physical parameters during NLCs preparation at 15,000 rpm homogenization speed for 5 mins was studied. Increasing Polysorbate 80 concentration from 0.75 to 2.0% w/v decreased PS significantly ($p < 0.05$) from 384.4 ± 7.9 to 142.3 ± 3.9 nm for oleic acid-based NLC placebos (P1-P4, P9) compared to a decrease in PS from 420.2 ± 12.2 to 225.2 ± 10.2 nm for castor oil-based NLC placebos (P5-P8), as shown in Table 1. However, no significant change in the PDI and ZP ($p > 0.05$) was observed. The decrease in PS could be attributed to the significant decrease in surface tension and surface free energy produced during homogenization.¹⁷

Table 1 Effect of Different Concentrations of Polysorbate 80 on Particle Size, Polydispersity Index, and Zeta Potential of Different NLC Placebos (Mean \pm SD, $n = 3$)

Formulation Composition (%w/v)	P1	P2	P3	P4	P5	P6	P7	P8
Glyceryl distearate	3.0	3.0	3.0	3.0	3.0	3.0	3.0	3.0
Oleic acid	1.0	1.0	1.0	1.0	–	–	–	–
Castor oil	–	–	–	–				
Polysorbate 80	0.75	1.0	1.5	2.0	0.75	1.0	1.5	2.0
Poloxamer 188	0.25	0.25	0.25	0.25	0.25	0.25	0.25	0.25
Glycerin	2.25	2.25	2.25	2.25	2.25	2.25	2.25	2.25
Water up to (mL)	10	10	10	10	10	10	10	10
Particle size (nm)	384.4 ± 7.9	291.6 ± 10.4	211.7 ± 4.5	142.3 ± 3.9	420.2 ± 12.2	352.5 ± 5.4	261.3 ± 6.5	225.2 ± 10.2
Polydispersity index	0.41 ± 0.06	0.42 ± 0.08	0.39 ± 0.02	0.38 ± 0.01	0.55 ± 0.07	0.55 ± 0.02	0.59 ± 0.03	0.57 ± 0.09
Zeta potential (mV)	-28.5 ± 1.5	-29.6 ± 0.7	-31.4 ± 1.3	-27.1 ± 1.7	-29.2 ± 1.5	-27.4 ± 1.7	-32.3 ± 1.3	-31.6 ± 1.1

Abbreviation: P, placebo.

Effect of Different Homogenization Speeds

The effect of homogenization speed on oleic acid-based NLC placebo formulations with 2% w/v Polysorbate 80 was studied. Increasing homogenization speed (from 14,000 to 15,000) decreased PS significantly from 314.5 ± 5.7 to 142.3 ± 3.9 nm, and PDI from 0.49 ± 0.06 to 0.38 ± 0.01 . There was no significant change in ZP. Moreover, increasing homogenization speed above 15,000 resulted in the blackening of the formulation, which could be attributed to the charring of lipids due to very high shear energy. Therefore, 15,000 rpm was selected as the optimal speed for the homogenization step during NLC preparation.

Effect of Total Lipids to Surfactant Ratio

The effect of increasing lipid to surfactant ratio for the NLC placebos composed of glyceryl distearate and oleic acid is shown in Table 2. Increasing total lipid to surfactant ratio (2:1 (P4) to 3:1 (P9)) significantly increased PS from 142.3 ± 3.9 to 226.0 ± 11.2 nm. At the same time, PDI increased from 0.38 ± 0.01 to 0.60 ± 0.05 . However, no significant change in ZP was observed. This observation could be due to the increase in the viscosity of the formulation on increasing the amount of lipid, which could make the applied shear during homogenization insufficient for further size reduction.²⁹ Therefore, a 2:1 total lipid to surfactant ratio was selected for the preparation of dual drug-loaded NLCs.

Preparation and Physical Characterization of NLCs

Following the physical characterization of the nine different placebos, P4 and P8 formulations were selected for dual drug loading as shown in Table 3. NT drug load was selected based on our earlier investigations by Patil et al, wherein the NT-NLCs prepared with 0.3% w/v NT drug load achieved higher drug concentrations into the posterior ocular tissues compared to commercial natamycin eye drops during in vivo ocular biodistribution studies in male New Zealand white albino rabbits.⁹ CIP drug load was also selected based on our earlier investigations by Youssef et al, wherein the transcorneal flux and permeability of the drug (0.1% w/v) from CIP-NLCs were improved by 4.0- and 3.5-fold, respectively when compared to the commercial eye drops.¹⁷

Oleic acid-based NLC (F1) showed significantly lower PS and PDI values than castor oil-based NLC dispersions (F2) which could be due to the single hydrocarbon chain of oleic acid compared to the branched triglyceride structure of castor oil. The ZP values were however not affected. This observation was consistent with earlier reports.³⁰ Although EE of NT was not affected ($p > 0.05$) by the type of liquid lipid used for NLC preparation, the EE of CIP decreased significantly ($p < 0.05$) in the F2 formulation. Therefore, the F1 formulation was selected for stability evaluation based on its smaller PS and narrower PDI, and because of the high EE achieved for both drugs.

Table 2 Effect of Total Lipid to Polysorbate 80 Ratio (2:1 and 3:1) on Particle Size, Polydispersity Index, and Zeta Potential of NLC Placebos, Composed of Glyceryl Distearate and Oleic Acid (Mean \pm SD, n = 3)

Formulation Composition (%w/v)	P4	P9
Glyceryldistearate	3.0	4.5
Oleic acid	1.0	1.5
Polysorbate 80	2.0	2.0
Poloxamer 188	0.25	0.25
Glycerin	2.25	2.25
Water up to (mL)	10	10
Particle size (nm)	142.3 ± 3.9	226.0 ± 11.2
Polydispersity index	0.38 ± 0.01	0.60 ± 0.05
Zeta potential (mV)	-27.1 ± 1.7	-27.8 ± 0.5

Abbreviation: P, placebo.

Table 3 Effect of Liquid Lipid on Particle Size, Polydispersity Index, Zeta Potential, % Drug Content, and % Entrapment Efficiency (Mean \pm SD, n = 3)

Formulation Composition (%w/v)		F1	F2
Ciprofloxacin		0.1	0.1
Natamycin		0.3	0.3
Glyceryldistearate		3.0	3.0
Oleic acid		1.0	–
Castor oil		–	1.0
Polysorbate 80		2.0	2.0
Poloxamer 188		0.25	0.25
Glycerin		2.25	2.25
Water up to (mL)		10	10
Particle size (nm)		196.2 \pm 1.2	283.4 \pm 4.2
Polydispersity index		0.43 \pm 0.06	0.66 \pm 0.03
Zeta potential (mV)		–28.1 \pm 1.4	–29.1 \pm 2.4
Drug content (%)	CIP	102.9 \pm 3.0	98.9 \pm 2.6
	NT	100.9 \pm 2.8	98.7 \pm 4.3
Entrapment efficiency (%)	CIP	80.9 \pm 2.9	19.2 \pm 2.2
	NT	98.7 \pm 1.9	95.5 \pm 2.5

Assay and EE for CIP-NT-NLCs

In the preparation of NLC formulations, the drug molecules need to be dissolved or dispersed in the oily phase, prior to the homogenization process, to obtain maximum drug entrapment and prevent drug precipitation post-preparation of the lipid-based nanocarriers.³¹ Moreover, higher EE is obtained with NLCs, compared to SLNs, due to the blend of solid and liquid lipids creating a disordered crystalline structure that provides higher space for more drug loading.³² Higher EE of CIP in F1 formulation (80.9 \pm 2.9) compared to F2 formulation (19.2 \pm 2.2) could be due to higher solubility of CIP in oleic acid compared to castor oil. However, higher EE of NT in both F1 and F2 formulations suggests that the EE of NT is highly dependent on solid lipid glyceryl distearate because NT is not soluble in oleic acid and this is in agreement with an earlier report.^{9,10} F1 and F2 formulations showed a % CIP content of 102.9 \pm 3.0 and 98.9 \pm 2.6, respectively. For NT, F1 and F2 formulations showed % NT content of 100.9 \pm 2.8 and 98.7 \pm 4.3, respectively, as shown in Table 3.

Stability of CIP-NT-NLCs

PS, PDI, and ZP are considered as good indicators of physical stability, while drug content is a good indicator of the chemical stability of the NLCs dispersion. Moreover, EE is also regarded as a good indicator of the physicochemical stability of the solid crystalline core. The physicochemical stability of the F1 formulation was determined by the storage of these colloidal dispersions at RF and RT for 90 days. The formulation did not show any aggregation or cracking, upon visual inspection, for 90 days (last-time point tested) at both storage conditions. Some changes, but statistically insignificant, were observed in PS, ZP, PDI, % assay, and % EE values, as shown in Figure 1. This demonstrates that the NLC formulations were stable at both RF and RT conditions. The stability of the formulation could be due to the electrostatic repulsion, which is the main requirement for the stability of lipid NPs, as well as the use of steric stabilizers.¹⁷

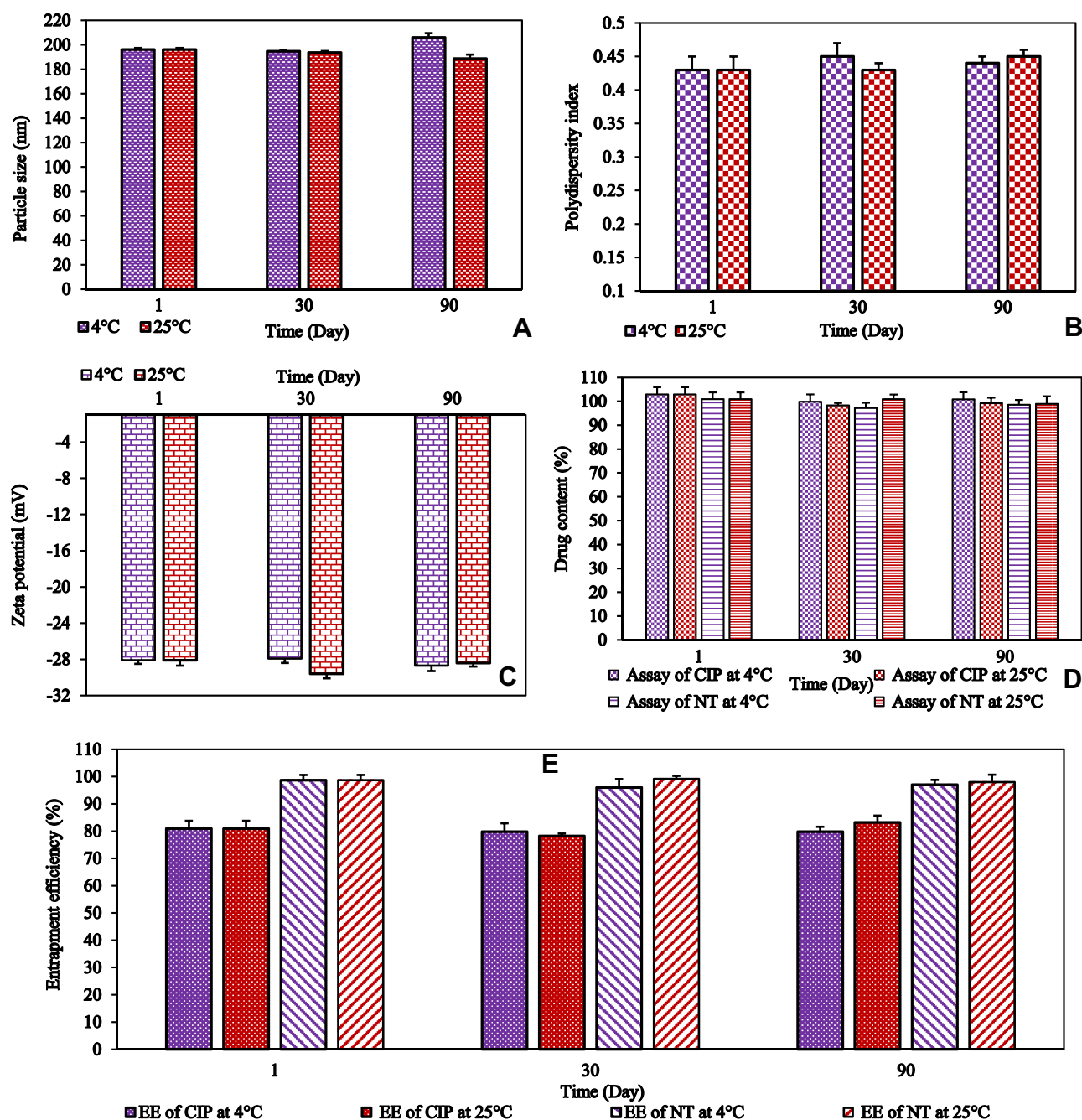


Figure 1 (A) particle size (PS), (B) polydispersity index (PDI), (C) zeta potential (ZP), (D) drug content of ciprofloxacin and natamycin, and (E) entrapment efficiency (EE) of ciprofloxacin and natamycin for FI formulation over three months storage at 4°C and 25°C (mean \pm SD, n = 3).

Characterization of CIP-NT-NLC-IG

Gellan gum is one of the most promising in-situ gelling polymers applicable in pharmaceutical technology.³³ Gellan gum (Gelrite®) is commercially available in the market as a low-acetyl gellan gum grade, this polymer undergoes gelation in the presence of mono and/or divalent cations.³³ Na⁺, Mg²⁺, and Ca²⁺ cations are naturally present in the tear fluid and induce gel formation of this polymer upon instillation as a liquid formulation into the *cul-de-sac*.³³ Gellan gum-based in situ gelling systems have been utilized in the formulation development of many drugs such as timolol maleate,³⁴ CIP hydrochloride,³⁵ and indomethacin.³⁶ The critical parameters to be considered during the application of gels for the

ocular surface are GT and GRT; lower GT is required to reduce loss due to tear turnover, and longer GRT is required for prolonged precorneal residence time. In the ocular milieu, GT <5 secs has been reported as an immediate sol-to-gel phase transition for ocular sol-to-gel transforming systems because the interblink time has an average of 4.0 ± 2.0 secs in normal individuals.³⁷ The thickening property of gellan gum is due to the aggregation of the double helices, achieved by decreased repulsion owing to mono or divalent cation binding to the helices in specific coordination sites around the carboxylate groups of the polymer, resulting in the rapid formation of an intact hydrogel matrix by cross-linking, and these mono and divalent cations are abundant in tear fluid.³⁸

F1-IG systems were prepared by adding various amounts of gellan gum (0.2, 0.3, and 0.4% w/v) to NLCs and the IG systems were evaluated based on rheological properties as shown in Table 4. GT of all F1-IG formulations was instantaneous, and GRT was more than 24 h for all tested gellan gum concentrations. A viscosity up to 50 cP allows easy topical ocular application.³⁹ The viscosity of F1-IG3 and F1-IG4 formulations was not in the range of commercial ophthalmic solutions in the absence of STF. The viscosity of the F1-IG2 formulation was found to be the lowest in the presence (22.3 ± 0.1 cP) and absence of STF (11.2 ± 0.2 cP). Therefore, F1-IG2 formulation was considered as the optimized IG formulation for further studies.

Stability Studies of the Optimized CIP-NT-NLC-IG

The stability of the F1-IG2 formulation was studied for a month at RT storage conditions, and the viscosity data is presented in Figure 2. This formulation showed a good stability profile with respect to viscosity, GT, and GRT during one-month storage at room temperature. There was no significant change ($p > 0.05$) in the viscosity of the formulation was also observed. Therefore, this formulation was further evaluated for in vitro release and ex vivo transcorneal permeation studies.

FTIR Studies

FTIR spectra were collected for pure CIP, pure NT, pure glyceryl distearate, oleic acid, physical mixture (CIP, NT, oleic acid, and glyceryl distearate), P4, and F1 formulations, to check for any incompatibility between the excipients and actives during and after preparation of nanodispersions (Figure 3). There were no peaks observed for both drugs in the physical mixture spectrum due to the high solubility of both drugs in liquid and solid lipids. Blank (placebo) and dual drug-loaded NLCs displayed a similar spectrum with a broad O-H stretching band at $3200\text{--}3600\text{ cm}^{-1}$ which is due to the external phase (H_2O). The FTIR did not show any characteristic peaks for both drugs in the NLC formulation due to the solubilization of the drug within the lipid matrix; the observed peaks were characteristic of some functional groups of the lipid excipients.

TEM

TEM micrographs obtained for F1 and F1-IG2 formulation revealed spherical shape. Moreover, no aggregation of NLCs particles was observed (Figure 4). Furthermore, the PS of NLCs was found to be less than 200 nm which is in a close agreement with the PS obtained with Zetasizer.

Table 4 The Viscosity of F1 and F1-IG Formulations with Different Gellan Gum Concentrations (mean \pm SD, n = 3)

Formulation	Gellan Gum (% w/v)	GT	GRT (h)	η without STF (cP)	η with STF (cP)
F1	0.0	NA	NA	4.9 ± 0.1	5.1 ± 0.1
F1-IG2	0.2	Immediate	>24	11.2 ± 0.2	22.3 ± 0.1
F1-IG3	0.3	Immediate	>24	75.9 ± 2.8	308.4 ± 4.4
F1-IG4	0.4	Immediate	>24	128.0 ± 6.7	800.0 ± 10.2

Abbreviations: GT, gelation time; GRT, gel residence time.

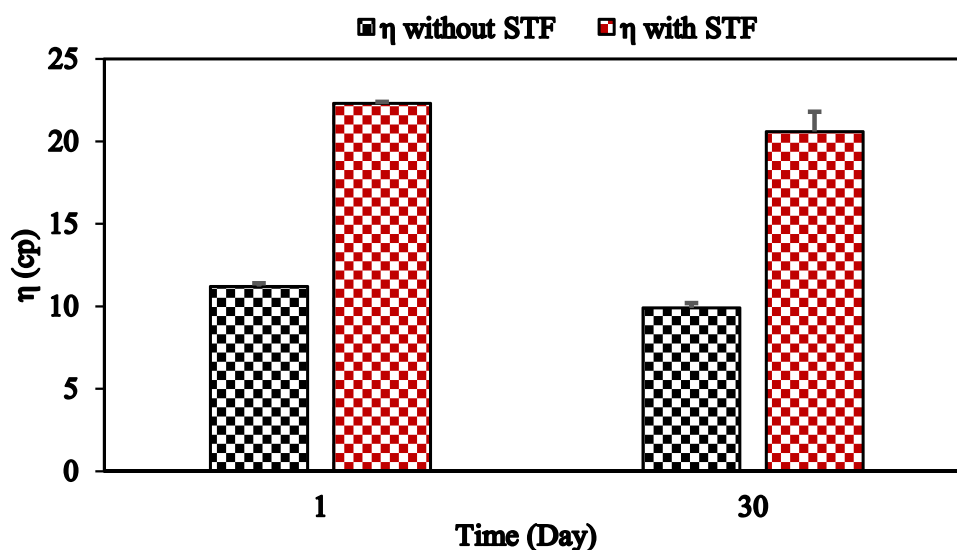


Figure 2 Viscosity of F1-IG2 formulation in the presence and absence of STF following one-month storage at 25°C (mean \pm SD, $n = 3$).

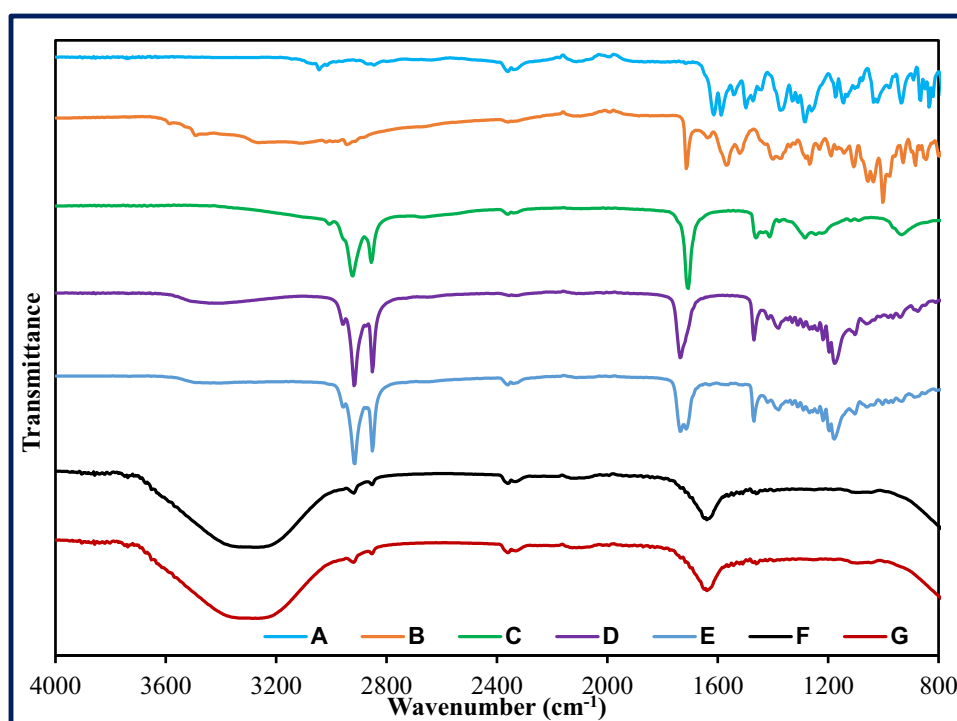


Figure 3 FTIR spectra of (A) ciprofloxacin, (B) natamycin, (C) oleic acid, (D) Glyceryl distearate, (E) physical mixture (ciprofloxacin, natamycin, oleic acid and glyceryl distearate), (F) placebo NLC (P4), and (G) NLC formulation (F1).

In vitro Release Studies

The in vitro release of CIP and NT from F1, F1-IG2, CIP-HCl-C, and NT-C formulations were evaluated by the dialysis method, and data is presented in Figure 5. The percentage cumulative release of CIP from CIP-HCL-C, F1, and F1-IG2 were $91.5 \pm 1.4\%$, $80.5 \pm 3.2\%$, and $65.3 \pm 4.0\%$, respectively within the time course of the experiment (24 h). CIP-HCl-C solution release data was reproducible with the earlier reported release studies.¹⁷ The overall cumulative percentage release of NT from NT-C, F1, and F1-IG2 were 74.5 ± 2.6 , 49.3 ± 2.4 , and $25.2 \pm 2.0\%$, respectively. Thus, both F1 and F1-IG2

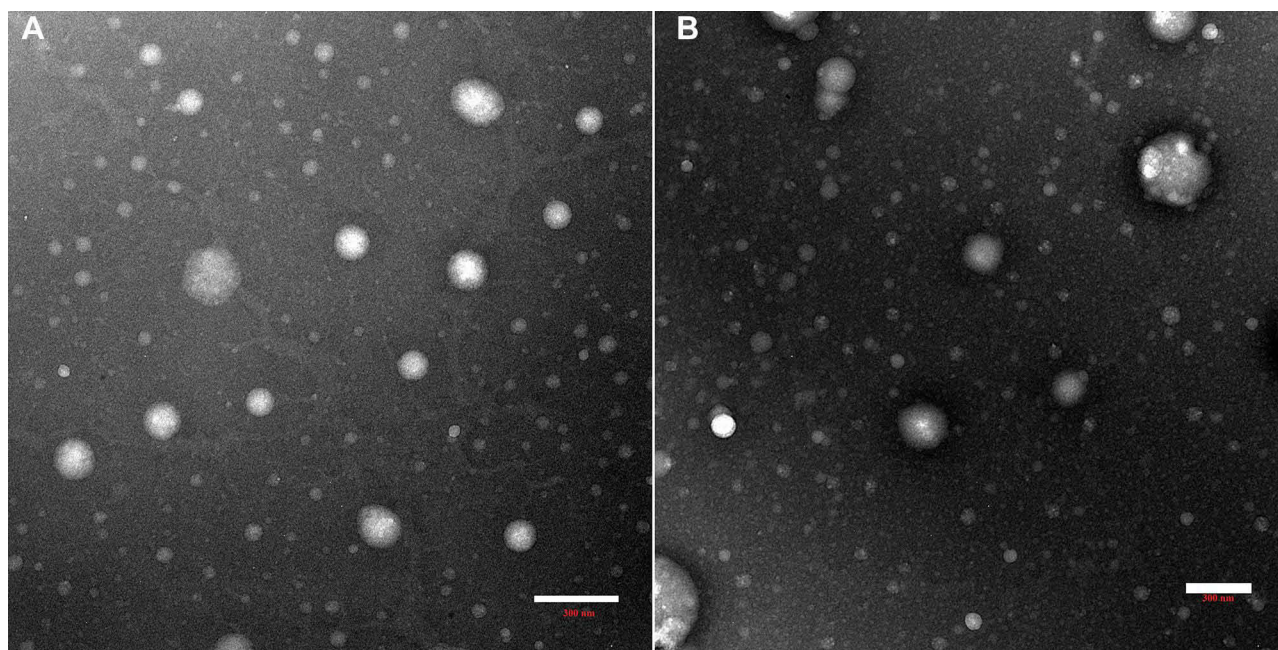


Figure 4 Transmission electron micrographs of F1 (A) and F1-IG2 (B) formulations.

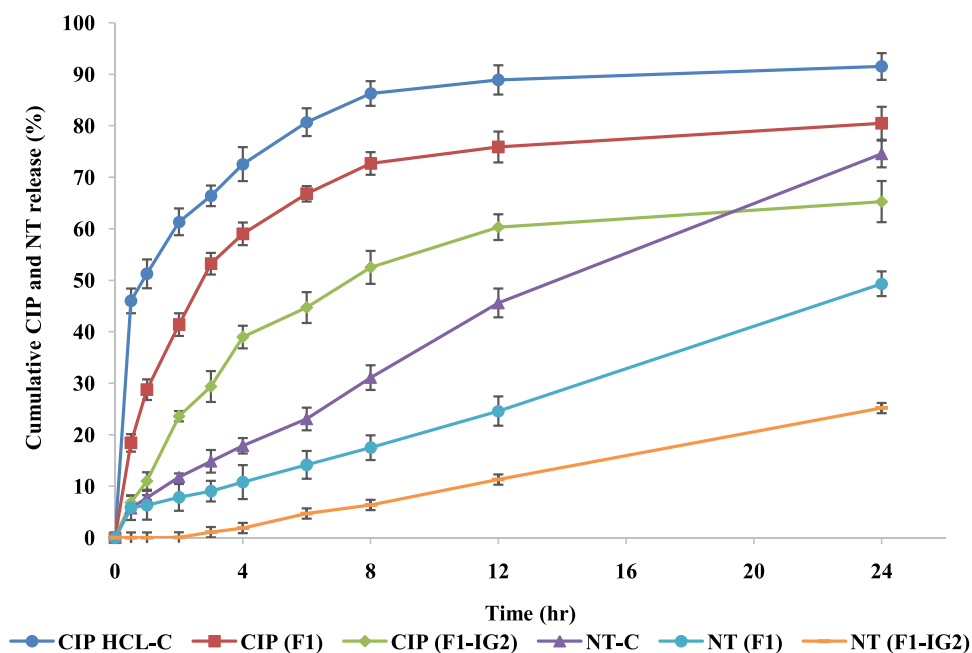


Figure 5 In vitro release of ciprofloxacin and natamycin from F1, F1-IG2, NT-C, and CIP-HCL-C formulations through thermo scientific™ slide-A-lyzer™ MINI dialysis device (10K MWCO) (mean \pm SD, n = 3).

formulations sustained the release of both drugs compared to the corresponding control formulations. CIP and NT are lipophilic drugs, and this could be a reason for the sustained release behavior from the lipid matrix of NLC and NLC-IG formulations. Moreover, sustained drug release profiles from the core crystalline lipid matrix could also be due to both drugs being embedded and entrapped in the core solid lipid matrix which leads to extended drug release.⁴⁰

Table 5 Mathematical Model Fitting of Release Kinetics of Ciprofloxacin and Natamycin from F1 and F1-IG2 Formulations (Mean \pm SD, n = 3)

Equation	$Q_0-Q = kt$	$\ln Q = kt$	$Q_0-Q = kt^{1/2}$	$\log (Q_0-Q) = n\log t + \log k$	
Coefficient of determination (R^2)					
Formulation	Zero-order	First-order	Higuchi	Korsmeyer-Peppas	
				R^2	n
CIP					
FI	0.8756	0.9561	0.9908	0.9989	0.54
FI-IG2	0.8935	0.9566	0.9795	0.9897	0.57
NT					
FI	0.9897	0.9796	0.9043	0.9911	0.83
FI-IG2	0.9887	0.9828	0.8340	0.9977	1.2

Notes: Where, Q_0 and Q represent initial drug content at the time t_0 and drug content at time t , respectively; Zero-order model: % drug released vs time; First order model: amount drug remaining vs time; Higuchi model: % drug released vs square root of time; Korsmeyer–Peppas model: log % drug released vs log time.

To predict the possible release pattern from the F1, F1-IG2, NT-C, and CIP-HCL-C formulations, the release data were analyzed using different release models; Zero-order, First-order, Higuchi matrix, and Korsmeyer–Peppas to check the goodness of fit.⁴¹ The R^2 value for each model is shown in Table 5. For CIP, the highest R^2 value was observed for Korsmeyer–Peppas model, followed by the Higuchi's, First-order, and Zero-order models for both formulations (F1, F1-IG2). For NT release from both formulations, the highest R^2 value was also observed with the Korsmeyer–Peppas model, followed by the zero-order, first-order, and Higuchi's models. All calculated slope values (n) of the Korsmeyer–Peppas model for both drugs from NLC and NLC-IG formulations indicated non-Fickian or anomalous drug release profiles, controlled by erosion and diffusion release mechanisms for NLCs and NLC-loaded hydrogels.⁴²

Kowalski et al studied the CIP MIC₉₀ values against 177 MK isolates. For fluoroquinolone-resistant *Staphylococcus aureus*, the MIC₉₀ value of CIP was 64 $\mu\text{g/mL}$, while the MIC₉₀ value against *Pseudomonas aeruginosa* was 0.125 $\mu\text{g/mL}$.⁴³ The data from the release studies reveal that the CIP content in the receiver solutions, obtained from both formulations – 184 $\mu\text{g/mL}$ from NLC and 110 $\mu\text{g/mL}$ from NLC-IG – was above the MIC₉₀ values against both types of bacteria, from the very first time point (30 min). The MIC₉₀ of NT is reported to be in the range of 1.56 to 6.25 $\mu\text{g/mL}$ against *Fusarium* species,⁴⁴ and 0.25 to 4.0 $\mu\text{g/mL}$ against *Candida* species.⁴⁵ The data from the release studies reveal that within 30 min the NT concentration achieved from the NLC formulation (174 $\mu\text{g/mL}$), was higher than the MIC₉₀ against both fungal species. However, from the NLC-IG formulation, NT concentration (30 $\mu\text{g/mL}$) exceeded the MIC₉₀ values only after the third hour. The presence of lipid metabolizing enzymes within the ocular tissue could improve NT release from the lipid matrix and achieve the MIC of the drug within the first 30 min after topical application.

Ex vivo Transcorneal Permeation Studies

Despite having a nictitating membrane and very low blinking frequency, the rabbit eye is generally considered the reference animal model for ocular experiments because of several similarities between the rabbit's eye anatomy and the anatomy of the human eye.⁴⁶ It is relatively easy to use compared to porcine or bovine models for both ex vivo and in vivo studies; therefore, it is useful for establishing ex vivo-in vivo correlations.⁴⁶ The transcorneal flux and permeability coefficient of test and control formulations are shown in Figure 6. The transcorneal flux and permeability of CIP from F1 and F1-IG2 formulations were 3.8- and 2.0-fold, and 4.0- and 2.2-fold higher, respectively, compared to the CIP-HCL-C. The transcorneal flux and permeability of NT from F1 and F1-IG2 formulations were 4.5- and 2.3-fold, and 5.0- and 2.5-fold higher, respectively, compared to the NT-C formulation.

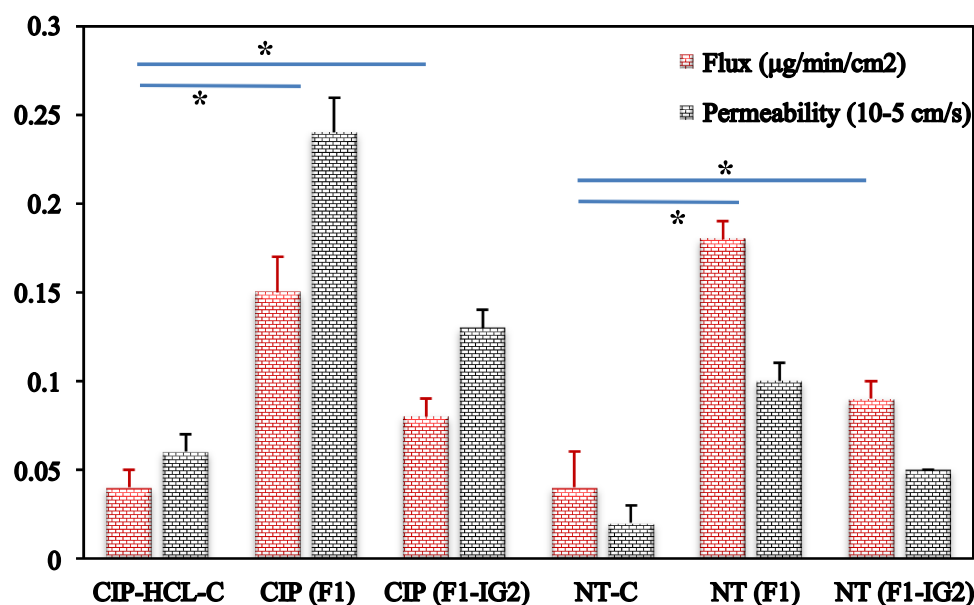


Figure 6 Transcorneal flux and permeability of ciprofloxacin and natamycin from F1, F1-IG2, NT-C, and CIP-HCL-C formulations through the isolated rabbit cornea (mean \pm SD, $n = 3$, *; means significant difference compared to control formulation).

The transcorneal flux of CIP and NT from F1 formulation was 1.9- and 2.0-fold higher, respectively, compared to that from the F1-IG2 formulation. The permeation data complements the data from the release study with the IG formulation displaying a more sustained release profile, thereby leading to lower transcorneal flux for both drugs.

NLCs are capable of enhancing ocular drug permeation through the cornea because their lipid components may interact with the oily layer of the tear film, allowing nanocarriers to remain in the conjunctival sac for a long time, where they act as a drug depot and resist washing away by continuous tear fluid drainage.⁴⁷ These nanocarriers can also form a film on the ocular surface, allowing the sustained release of the loaded drugs.¹⁷ Furthermore, nanocarriers below 200 nm could be internalized by a receptor-mediated endocytosis uptake mechanism through the corneal cells.⁴⁸ Gellan gum is utilized as an ion-sensitive gelling agent for different medical uses. Higher mucoadhesion of polymer with cellular glycoproteins through hydrophobic interactions/van der Waals forces/ionic/hydrogen bonding leads to prolonged contact time of hydrogel with the ocular surface, resulting in enhanced ocular drug penetration.⁴⁹

Conclusion

Dual drug-loaded NLCs and their IG formulations were successfully prepared, using gellan gum as an in-situ gelling agent. NLC and NLC-IG formulations exhibited physical and chemical stability for three- and one month, respectively at conditions tested. An effective sustained release profile, and enhanced transcorneal permeability and flux of both drugs was observed when compared to the control formulations. Thus, NLC and its in-situ gel formulations could be used to co-deliver of CIP and NT for the treatment of mixed ocular infections or for empirical treatment in case of limited access to health care diagnostic services.

Data Sharing Statement

The data presented in this study are available upon request from the corresponding author.

Funding

This project was supported in part by grant #P30GM122733 from the National Institute of General Medical Sciences, National Institutes of Health. The content is solely the responsibility of the authors and does not necessarily represent the official views of the National Institutes of Health.

Disclosure

The authors report no conflicts of interest in this work.

References

1. Ung L, Bispo PJM, Shanbhag SS, Gilmore MS, Chodosh J. The persistent dilemma of microbial keratitis: global burden, diagnosis, and antimicrobial resistance. *Surv Ophthalmol*. 2019;64(3):255–271. doi:10.1016/j.survophthal.2018.12.003
2. Collier SA, Gronostaj MP, MacGurn AK, et al. Estimated burden of keratitis—United States, 2010. *MMWR Morb Mortal Wkly Rep*. 2014;63(45):1027.
3. Ahn M, Yoon KC, Ryu SK, Cho NC, You IC. Clinical aspects and prognosis of mixed microbial (bacterial and fungal) keratitis. *Cornea*. 2011;30(4):409–413. doi:10.1097/ICO.0b013e3181f23704
4. Flinney GD, Pecan PE, Cathcart JN, Palestine AG. Trends in treatment strategies for suspected bacterial endophthalmitis. *Graefes Arch Clin Exp Ophthalmol*. 2018;256(4):833–838. doi:10.1007/s00417-018-3910-3
5. Basak SK, Basak S, Mohanta A, Bhowmick A. Epidemiological and microbiological diagnosis of suppurative keratitis in Gangetic West Bengal, Eastern India. *Indian J Ophthalmol*. 2005;53(1):17–22. doi:10.4103/0301-4738.15280
6. Gopinathan U, Sharma S, Garg P, Rao GN. Review of epidemiological features, microbiological diagnosis and treatment outcome of microbial keratitis: experience of over a decade. *Indian J Ophthalmol*. 2009;57(4):273–279. doi:10.4103/0301-4738.53051
7. Leck AK, Thomas PA, Hagan M, et al. Aetiology of suppurative corneal ulcers in Ghana and south India, and epidemiology of fungal keratitis. *BJO*. 2002;86(11):1211–1215. doi:10.1136/bjo.86.11.1211
8. Ho JW, Fernandez MM, Rebong RA, Carlson AN, Kim T, Afshari NA. Microbiological profiles of fungal keratitis: a 10-year study at a tertiary referral center. *J Ophthalmol Infect*. 2016;6(1):5. doi:10.1186/s12348-016-0071-6
9. Patil A, Lakhani P, Taskar P, et al. Formulation development, optimization, and in vitro–in vivo characterization of natamycin-loaded pegylated nano-lipid carriers for ocular applications. *J Pharm Sci*. 2018;107(8):2160–2171. doi:10.1016/j.xphs.2018.04.014
10. Patil A, Lakhani P, Taskar P, Avula B, Majumdar S. Carboxyvinyl polymer and guar-borate gelling system containing natamycin loaded pegylated nanolipid carriers exhibit improved ocular pharmacokinetic parameters. *J Ocul Pharmacol Ther*. 2020;36(6):410–420. doi:10.1089/jop.2019.0140
11. Miller D. Update on the epidemiology and antibiotic resistance of ocular infections. *Middle East Afr J Ophthalmol*. 2017;24(1):30–42. doi:10.4103/meajo.MEAJO_276_16
12. Patel A, Cholkar K, Agrahari V, Mitra AK. Ocular drug delivery systems: an overview. *World J Pharmacol*. 2013;2(2):47–64. doi:10.5497/wjp.v2.i2.47
13. Balguri SP, Adelli GR, Janga KY, Bhagav P, Majumdar S. Ocular disposition of ciprofloxacin from topical, PEGylated nanostructured lipid carriers: effect of molecular weight and density of poly (ethylene) glycol. *Int J Pharm*. 2017;529(1):32–43. doi:10.1016/j.ijpharm.2017.06.042
14. Fong CF, Tseng CH, Hu FR, Wang IJ, Chen WL, Hou YC. Clinical characteristics of microbial keratitis in a university hospital in Taiwan. *Am J Ophthalmol*. 2004;137(2):329–336. doi:10.1016/j.ajo.2003.09.001
15. Shah A, Sachdev A, Coggon D, Hossain P. Geographic variations in microbial keratitis: an analysis of the peer-reviewed literature. *Br J Ophthalmol*. 2011;95(6):762–767. doi:10.1136/bjo.2009.169607
16. Youssef AAA, Cai C, Dudhipala N, Majumdar S. Design of topical ocular ciprofloxacin nanoemulsion for the management of bacterial keratitis. *Pharmaceutics*. 2021;14(3):210. doi:10.3390/ph14030210
17. Youssef A, Dudhipala N, Majumdar S. Ciprofloxacin loaded nanostructured lipid carriers incorporated into in-situ gels to improve management of bacterial endophthalmitis. *Pharmaceutics*. 2020;12(6):572. doi:10.3390/pharmaceutics12060572
18. Friedlaender MH. A review of the causes and treatment of bacterial and allergic conjunctivitis. *Clin Ther*. 1995;17(5):800–810. doi:10.1016/0149-2918(95)80058-1
19. Stergiopoulou T, Meletiadis J, Sein T, et al. Comparative pharmacodynamic interaction analysis between ciprofloxacin, moxifloxacin and levofloxacin and antifungal agents against *Candida albicans* and *Aspergillus fumigatus*. *J Antimicrob Chemother*. 2009;63(2):343–348. doi:10.1093/jac/dkn473
20. Janga KY, Tatke A, Dudhipala N, et al. Gellan gum based *sol-to-gel* transforming system of natamycin transfersomes improves topical ocular delivery. *J Pharmacol Exp Ther*. 2019;370(3):814–822. doi:10.1124/jpet.119.256446
21. Janga KY, Tatke A, Balguri SP, et al. Ion-sensitive *in situ* hydrogels of natamycin bilosomes for enhanced and prolonged ocular pharmacotherapy: *in vitro* permeability, cytotoxicity and *in vivo* evaluation. *Artif Cells Nanomed Biotechnol*. 2018;46(sup1):1039–1050. doi:10.1080/21691401.2018.1443117
22. Tatke A, Dudhipala N, Janga KY, et al. In situ gel of triamcinolone acetate-loaded solid lipid nanoparticles for improved topical ocular delivery: tear kinetics and ocular disposition studies. *Nanomaterials*. 2019;9(1):33. doi:10.3390/nano9010033
23. Ali M, Byrne ME. Challenges and solutions in topical ocular drug-delivery systems. *Expert Rev Clin Pharmacol*. 2008;1(1):145–161. doi:10.1586/17512433.1.1.145
24. Dudhipala N, Ali Youssef AA, Banala N. Colloidal lipid nanodispersion enriched hydrogel of antifungal agent for management of fungal infections: comparative in-vitro, ex-vivo and in-vivo evaluation for oral and topical application. *Chem Phys Lipids*. 2020;233:104981. doi:10.1016/j.chemphyslip.2020.104981
25. Farid RM, El-Salamouni NS, El-Kamel AH, El-Gamal SS. Chapter 16 - Lipid-based nanocarriers for ocular drug delivery. In: Andronesu E, Grumezescu AM editors. *Nanostructures for Drug Delivery*. Micro and Nano Technologies Elsevier; 2017:495–522. doi:10.1016/B978-0-323-46143-6.00016-6
26. Dudhipala N, Ay AA. Amelioration of ketoconazole in lipid nanoparticles for enhanced antifungal activity and bioavailability through oral administration for management of fungal infections. *Chem Phys Lipids*. 2020;232:104953. doi:10.1016/j.chemphyslip.2020.104953
27. Müller RH, Radtke M, Wissing SA. Solid lipid nanoparticles (SLN) and nanostructured lipid carriers (NLC) in cosmetic and dermatological preparations. *Adv Drug Deliv Rev*. 2002;54:S131–S155. doi:10.1016/S0169-409X(02)00118-7
28. Agrahari V, Mandal A, Agrahari V, et al. A comprehensive insight on ocular pharmacokinetics. *Drug Deliv and Transl Res*. 2016;6(6):735–754. doi:10.1007/s13346-016-0339-2

29. Ghadiri M, Fatemi S, Vatanara A, et al. Loading hydrophilic drug in solid lipid media as nanoparticles: statistical modeling of entrapment efficiency and particle size. *Int J Pharm.* **2012**;424(1–2):128–137. doi:10.1016/j.ijpharm.2011.12.037
30. Cirri M, Maestrini L, Maestrelli F, et al. Design, characterization and in vivo evaluation of nanostructured lipid carriers (NLC) as a new drug delivery system for hydrochlorothiazide oral administration in pediatric therapy. *Drug Deliv.* **2018**;25(1):1910–1921. doi:10.1080/10717544.2018.1529209
31. Zur Mühlen A, Schwarz C, Mehnert W. Solid lipid nanoparticles (SLN) for controlled drug delivery – drug release and release mechanism. *Eur J Pharm Biopharm.* **1998**;45(2):149–155. doi:10.1016/S0939-6411(97)00150-1
32. Dudhipala N, Janga KY, Gorre T. Comparative study of nisoldipine-loaded nanostructured lipid carriers and solid lipid nanoparticles for oral delivery: preparation, characterization, permeation and pharmacokinetic evaluation. *Artif Cells, Nanomed Biotechnol.* **2018**;46(sup2):616–625. doi:10.1080/21691401.2018.1465068
33. Wu Y, Liu Y, Li X, et al. Research progress of in-situ gelling ophthalmic drug delivery system. *AJPS.* **2019**;14(1):1–15. doi:10.1016/j.ajps.2018.04.008
34. Rozier A, Mazuel C, Grove J, Plazonnet B. Gelrite®: a novel, ion-activated, in-situ gelling polymer for ophthalmic vehicles. Effect on bioavailability of timolol. *Int J Pharm.* **1989**;57(2):163–168. doi:10.1016/0378-5173(89)90305-0
35. Balasubramaniam J, Pandit JK. Ion-activated in situ gelling systems for sustained ophthalmic delivery of ciprofloxacin hydrochloride. *Drug Deliv.* **2003**;10(3):185–191. doi:10.1080/713840402
36. Balasubramaniam J, Kant S, Pandit JK. In vitro and in vivo evaluation of the gelrite gellan gum-based ocular delivery system for indomethacin. *Acta Pharm.* **2003**;53(4):251–261.
37. Tomlinson A, Khanal S. Assessment of tear film dynamics: quantification approach. *Ocul Surf.* **2005**;3(2):81–95. doi:10.1016/S1542-0124(12)70157-X
38. Morris ER, Nishinari K, Rinaudo M. Gelation of gellan – a review. *Food Hydrocoll.* **2012**;28(2):373–411. doi:10.1016/j.foodhyd.2012.01.004
39. Uddin M, Mamun AA, Kabir M, et al. Quality control tests for ophthalmic pharmaceuticals: pharmacopoeial standards and specifications. *JAMPS.* **2017**;14(2):1–17. doi:10.9734/JAMPS/2017/33924
40. Das S, Ng WK, Tan RBH. Are nanostructured lipid carriers (NLCs) better than solid lipid nanoparticles (SLNs): development, characterizations and comparative evaluations of clotrimazole-loaded SLNs and NLCs? *Eur J Pharm Sci.* **2012**;47(1):139–151. doi:10.1016/j.ejps.2012.05.010
41. Dudhipala N, Gorre T. Neuroprotective effect of ropinirole lipid nanoparticles enriched hydrogel for parkinson's disease: in vitro, ex vivo, pharmacokinetic and pharmacodynamic evaluation. *Pharmaceutics.* **2020**;12(5):448. doi:10.3390/pharmaceutics12050448
42. Siepmann J, Peppas NA. Modeling of drug release from delivery systems based on hydroxypropyl methylcellulose (HPMC). *Adv Drug Deliv Rev.* **2001**;64:19.
43. Kowalski RP, Dhaliwal DK, Karenchak LM, et al. Gatifloxacin and moxifloxacin: an in vitro susceptibility comparison to levofloxacin, ciprofloxacin, and ofloxacin using bacterial keratitis isolates. *Am J Ophthalmol.* **2003**;136(3):500–505. doi:10.1016/S0002-9394(03)00294-0
44. Sharma N, Chacko J, Velpandian T, et al. Comparative evaluation of topical versus intrastromal voriconazole as an adjunct to natamycin in recalcitrant fungal keratitis. *Ophthalmology.* **2013**;120(4):677–681. doi:10.1016/j.ophtha.2012.09.023
45. Motukupally S, Nanapur V, Chathoth K, et al. Ocular infections caused by candida species: type of species, in vitro susceptibility and treatment outcome. *Indian J Med Microbiol.* **2015**;33(4):538–546. doi:10.4103/0255-0857.167331
46. Agarwal P, Rupenthal ID. In vitro and ex vivo corneal penetration and absorption models. *Drug Deliv and Transl Res.* **2016**;6(6):634–647. doi:10.1007/s13346-015-0275-6
47. Seyfoddin A, Al-Kassas R. Development of solid lipid nanoparticles and nanostructured lipid carriers for improving ocular delivery of Acyclovir. *Drug Dev Ind Pharm.* **2013**;39(4):508–519. doi:10.3109/03639045.2012.665460
48. Foster KA, Yazdani M, Audus KL. Microparticulate uptake mechanisms of in-vitro cell culture models of the respiratory epithelium. *J Pharm Pharmacol.* **2001**;53(1):57–66. doi:10.1211/0022357011775190
49. Serra L, Doménech J, Peppas N. Engineering design and molecular dynamics of mucoadhesive drug delivery systems as targeting agents. *Eur J Pharm Biopharm.* **2009**;71(3):519–528. doi:10.1016/j.ejpb.2008.09.022

International Journal of Nanomedicine

Dovepress

Publish your work in this journal

The International Journal of Nanomedicine is an international, peer-reviewed journal focusing on the application of nanotechnology in diagnostics, therapeutics, and drug delivery systems throughout the biomedical field. This journal is indexed on PubMed Central, MedLine, CAS, SciSearch®, Current Contents®/Clinical Medicine, Journal Citation Reports/Science Edition, EMBase, Scopus and the Elsevier Bibliographic databases. The manuscript management system is completely online and includes a very quick and fair peer-review system, which is all easy to use. Visit <http://www.dovepress.com/testimonials.php> to read real quotes from published authors.

Submit your manuscript here: <https://www.dovepress.com/international-journal-of-nanomedicine-journal>